The Electronic Spectrum of the Prephenate Dianion. An Experimental and Theoretical (MD/QM) Comparison

Adrian E. Roitberg,*,† Sharon E. Worthington,‡ Marcia J. Holden,† Martin P. Mayhew,† and Morris Krauss‡,†

Contribution from the Biotechnology Division, National Institute for Standards and Technology, 100 Bureau Drive, Stop 8312, Gaithersburg, Maryland 20899-8312, and Center for Advanced Research in Biotechnology, 9600 Gudelsky Drive, Rockville, Maryland, 20850

Received December 30, 1999. Revised Manuscript Received May 18, 2000

Abstract: Prephenate is the product of a Claisen rearrangement of chorismate. The enzyme chorismate mutase (CM from *B. subtilis*) accelerates the reaction by a factor of 10^6. The standard method for quantifying prephenate measures the electronic absorption spectrum after acid conversion to phenylpyruvate and subsequent alkaline treatment. To the best of our knowledge, there is no reported UV/Vis spectrum for pure prephenate. The present experimental measurement thus solves this lack of data. A novel molecular dynamics/quantum mechanics method was used to theoretically compute the electronic spectrum, and was used as supporting analysis for the new experimental spectrum. The agreement between theory and experiment is excellent in the position of the absorption peaks, their relative intensities, and their widths. A number of prephenate conformers are possible in aqueous solution, with the active conformer of CM binding just one conformer which is analogous to the dominant conformer in solution. The conformers are studied in vacuo and in the enzyme active site by ab initio quantum chemical calculations, and in solution with a classical molecular dynamics simulation. The data presented here also suggest that the electronic spectrum of prephenate bound to the chorismate mutase active site should be observed, even in the presence of other members of the aromatic amino acid pathway.

Introduction

Prephenate is the product of a Claisen rearrangement of chorismate. The enzyme chorismate mutase (CM) accelerates the reaction by a factor of 10^6 in *B. subtilis*.[1] This reaction is the first major branch point in the metabolic pathway leading to the synthesis of the aromatic amino acids phenylalanine and tyrosine in bacteria, plants, and fungi, but not in mammals.[2]

NMR studies suggest that the rate-limiting step for the enzymatic reaction under the condition of prephenate saturation is the release of product.[3] Since the prephenate molecule spends considerable time inside the enzyme, a variety of spectroscopies can be used to study its interaction with the active site of CM. The IR spectrum of prephenate bound in the chorismate mutase from *B. subtilis* has been observed.[3] However, there is no direct report for the electronic spectrum of either free or CM-bound prephenate. The standard method for quantifying prephenate in solution[4−6] requires its conversion in acid media to phenylpyruvate followed by an alkaline treatment with 1 N NaOH. The absorption coefficient (ϵ) at 320 nm is reported at 17 500 M^{-1} cm^{-1} although there is no current knowledge as to the identity of the chemical entity responsible for this very large absorption. The extreme conditions suggested for the quantification of prephenate are inappropriate to use if we wish to follow the concentration of prephenate in the presence of an active enzyme.

Analysis of the prephenate structure suggests that its UV spectrum should be observable. Both prephenate and phenylpyruvate[5] present an analogous chromophore motif (a carbonyl contiguous to the carboxylate anion) suggesting that they should have a similar spectrum. We would then expect prephenate to absorb in the vicinity 330 nm.

Theoretical calculations of the electronic spectra of these molecules have not been done before but substantial literature exists on the Claisen rearrangement both in vacuo[7] and in the enzyme-catalyzed reaction.[8−11] A low-energy prephenate conformer has been reported[12] but this is not the structure determined in the active site of chorismate mutase.[13] Although it is certainly the global minimum in vacuo, we will show that in solution, the in vacuo reported structure[12] is comparable with, but higher in energy than others. In the reported structure[12] the hydroxyl makes a short hydrogen bond to the carboxyl substituent on the ring (see Figure 1b). The conformer bound in the enzyme-active site rotates the pyruvate above the ring with the hydroxyl also rotated so that its bond parallels the carbonyl bond (see Figure 1a).

* To whom correspondence should be addressed. E-mail: adrian@nist.gov.
† National Institute for Standards and Technology.
‡ Center for Advanced Research in Biotechnology.

(1) Gray, J. V.; Golinellipimpaneau, B.; Knowles, J. R. *Biochemistry* **1990**, *29*, 376−383.
(2) Knaggs, A. R. *Nat. Prod. Rep.* **1999**, *16*, 525−560.
(3) Gray, J. V.; Knowles, J. R. *Biochemistry* **1994**, *33*, 9953−9959.
(4) Gibson, F. *Biochem. J.* **1964**, *90*, 256.
(5) Gibson, M. I.; Gibson, F. *Biochem. J.* **1964**, *90*, 248.
(6) Connelly, J. A.; Siehl, D. L. *Methods Enzymol.* **1987**, *142*, 422−431.
(7) Wiest, O.; Houk, K. N. *J. Org. Chem.* **1994**, *59*, 7582−7584.
(8) Davidson, M. M.; Gould, I. R.; Hillier, I. H. *J. Chem. Soc., Chem. Commun.* **1995**, 63−64.
(9) Davidson, M. M.; Gould, I. R.; Hillier, I. H. *J. Chem. Soc., Perkin Trans. 2* **1996**, 525−532.
(10) Lyne, P. D.; Mulholland, A. J.; Richards, W. G. *J. Am. Chem. Soc.* **1995**, *117*, 11345−11350.
(11) Worthington, S. E.; Krauss, M. *Computers in Chemistry*. In Press.
(12) Kast, P.; Tewari, Y. B.; Wiest, O.; Hilvert, D.; Houk, K. N.; Goldberg, R. N. *J. Phys. Chem. B* **1997**, *101*, 10976−10982.
(13) Chook, Y. M.; Gray, J. V.; Ke, H. M.; Lipscomb, W. N. *J. Mol. Biol.* **1994**, *240*, 476−500.

10.1021/ja9945358 CCC: $19.00
Published on Web 07/15/2000

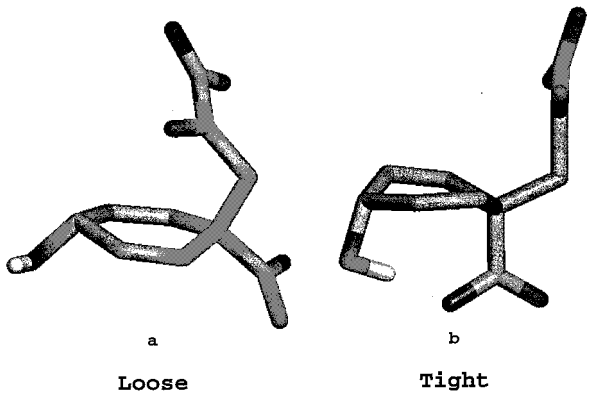

Figure 1. Two dominant conformers of prephenate in solution. Conformer a has both the OH and COO− groups solvated by the environment. Conformer b has a strong H-bond between the OH and the COO− groups.

In this paper, we will present a number of results: We will compute energetics and dynamics of prephenate under vacuum and in solution. The UV spectrum of pure prephenate in solution and inside CM's active site will be calculated and measured. A comparison of conformation and spectra between in vacuo and solution (and enzyme enviroment) will be carried out. The calculation of the spectra requires ab initio quantum methods while the determination of the population of solvated structures is done with classical molecular dynamics methods in explicit water. A continuum methodology to determine the solvation structure is not appropriate because the solute is a dianion interacting with the solvent through many strong ionic hydrogen bonds.

We will refer to the methodology used in this article as molecular dynamics-quantum mechanics (MD-QM). In this technique, one uses each tool sequentially, exploiting their particular strengths. Classical MD is a very fast and good sampling tool, while QM, being an accurate and more expensive representation of the system, is used only on a small number of snapshots extracted from the MD trajectory. This is analogous to the Monte Carlo-quantum mechanical method used by Couthino et al. for the treatment of solvent effects on electronic spectra.[14] The main difference in the procedures is the fact that Couthino et al. apply QM methods to uncorrelated frames from a MD run, while we use the MD trajectory to extract frames according to their relative weights. Another related use of MD-QM can be found in the work of Wood et al.[15] where configurations from a classical simulation (molecular dynamics or Monte Carlo) with empirical solute−solvent interactions are used to calculate free energies with quantum mechanically derived solute−solvent interactions.

The binding of prephenate in the active site of chorismate mutase (*B. subtilis*) is studied with the newly developed effective fragment potential (EFP) method.[16] Prephenate is described as an all-electron solute and the active site by the EFPs which represent the exchange repulsion, electrostatics, and polarization interactions between prephenate and the enzyme active site. The prephenate structure in the active site was quantum mechanically optimized in a model of the active site extracted from the X-ray structure for the *B. subtilis* enzyme.[13] The calculated spectra was computed for this optimized structure.

(14) Coutinho, K.; Canuto, S. *Adv. Quantum Chem.* **1997**, *28*, 89−105.
(15) Wood, R. H.; Yezdimer, E. M.; Sakane, S.; Barriocanal, J. A.; Doren, D. J. *J. Chem. Phys.* **1999**, *110*, 1329−1337.
(16) Day, P. N.; Jensen, J. H.; Gordon, M. S.; Webb, S. P.; Stevens, W. J.; Krauss, M.; Garmer, D.; Basch, H.; Cohen, D. *J. Chem. Phys.* **1996**, *105*, 1968−1986.

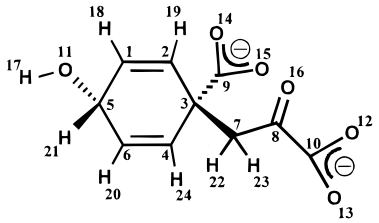

Figure 2. Diagram of the prephenate dianion with atom numbering.

Table 1. Atom Names, Types, and Charges Used for the Molecular Dynamics Runs

atom name	atom type (AT)	charge	atom name	atom type (AT)	charge
C1	CA	−0.1770	O13	O2	−0.7880
C2	CA	−0.2216	O14	O2	−0.7911
C3	CT	0.1669	O15	O2	−0.7911
C4	CA	−0.1620	O16	O	−0.5801
C5	CT	0.4885	H17	HO	0.4061
C6	CA	−0.3480	H18	HA	0.0906
C7	CT	0.0051	H19	HA	0.1345
C8	C	0.3783	H20	HA	0.1110
C9	C	0.7186	H21	H1	0.0205
C10	C	0.7329	H22	H1	0.0154
O11	OH	−0.7719	H23	H1	0.0154
O12	O2	−0.7880	H24	HA	0.1350

The previously reported FTIR spectrum for prephenate inside the active site of CM[3] was measured as a difference spectrum between the free and the product-bound enzyme. The existence of a UV spectrum of prephenate within the enzyme-active site now opens the possibility of using selective and sensitive spectral methods such as resonance Raman to directly determine the vibrational coupling between ligand and protein. This would be an example of the many types of spectroscopies of substrates bound in active sites that can be used to determine the properties of the native or mutant sites.

Methods

Molecular Dynamics. The molecular dynamics runs were performed using the program Amber, version 5.0.[17] A 6-31G** Hartree−Fock in vacuo calculation was done, and point charges assigned to the classical atoms based on a global fit to the electrostatic potential.[18] The overall charge of the molecule was −2. A diagram of prephenate is presented in Figure 2, while Table 1 shows the atom name, types, and charges derived as described above. Table 2 shows the bond, angle, and dihedral parameters not present in the standard force field.[19]

The prephenate molecule was built using Leap[20] with equilibrium values for the internal coordinates. The prephenate was immersed in a box of TIP3P waters. The wetting was set up such that at least 10 Å was available between the surface of the molecule and the box sides. At least 2 Å was left between the surface of the molecule and the closest O atom of any water molecule to prevent unfavorable overlaps. A total of 678 water molecules are added this way, producing a box of dimension 33.0 × 31.6 × 31.5 Å^3. The excess charge of prephenate (−2) was smeared into the whole system, resulting in a overall neutral charge. This procedure changes the per-atom charges by less than 0.1%. The system was heated from 0 K to 300 K over 100 ps, using periodic

(17) Case, D. A.; Pearlman, D. A.; Caldwell, J. W.; Cheatam, T. E., III; Ross, W. S.; Simmerling, C. L.; Darden, T. A.; Merz, K. M.; Stanton R. V.; Cheng A. L.; Vincent J. J.; Crowley M.; Ferguson D. M.; Radner R. J.; Seibel G. L.; Singh U. C.; Weiner P. K.; Kollman P. A. *Amber*, 5.0 ed.; University of California: San Francisco, 1997.
(18) Bayly, C. I.; Cieplak, P.; Cornell, W. D.; Kollman, P. A. *J. Phys. Chem.* **1993**, *97*, 10269−10280.
(19) Cornell, W. D.; Cieplak, P.; Bayly, C. I.; Gould, I. R.; Merz, K. M.; Ferguson, D. M.; Spellmeyer, D. C.; Fox, T.; Caldwell, J. W.; Kollman, P. A. *J. Am. Chem. Soc.* **1996**, *118*, 2309−2309.
(20) Schafmeister, C. E.; Ross, W. S.; Romanovski, V. *Leap*; University of California: San Francisco, 1995.

Table 2. Modifications to the Standard Amber 96 Parameter Set

Bonds		
AT1−AT2	force constant (kcal/mol/Å^2)	equilibrium dist (Å)
CA-CA	469.0	1.350
C−C	469.0	1.553

Angles		
AT1−AT2−AT3	force constant (kcal/mol/deg^2)	equilibrium angle (deg)
CA−CT−CA	70.0	109.5
CA−C−O2	70.0	120.0
HA−CA−HA	35.0	120.0
CA−CT−OH	50.0	109.5
H1−CT−CA	50.0	109.5
CT−CA−HA	50.0	120.0
CA−CT−C	63.0	109.5
CT−C−C	70.0	120.0
C−C−O2	70.0	120.0
C−C −O	70.0	120.0
C−CT−CA	50.0	109.5

Dihedrals				
AT1−AT2−AT3−AT4	IDIVF	PK (kcal/mol)	phase (deg)	PN
X−OS−CA−X	2	0.375	180.0	2
X−C−C−X	4	1.650	180.0	2

boundary conditions and a constant pressure algorithm (with a pressure relaxation time of 0.2 ps), and a particle mesh Ewald (PME) implementation of the Ewald sum for long-range electrostatics. A dielectric constant of 1 was used throughout. A spherical cutoff of 9 Å was used for the Lennard-Jones nonbonded potentials and the direct part of the Ewald sum calculation. The time step was 2 fs. The nonbonded list was updated every 20 fs. The bonds that involved a H atom were constrained to their equilibrium lengths by using the SHAKE method. After the heating period was completed, another 100 ps of equilibration were performed with the same set of parameters. During the equilibration period, the pressure stabilized around 1 atm and the temperature around 300 K. The final simulation box stabilized around $28.5 \times 27.3 \times 27.1$ Å^3, with a density around 0.98 g/cm^3. A total of 3.0 ns of dynamics were kept for analysis, with snapshots saved every 1 ps.

Quantum Calculation. All calculations used the GAMESS suite of quantum chemistry codes for both geometry optimizations and the calculation of the excitation energies.[21] All geometry optimizations were done at the restricted Hartree−Fock (RHF) level using effective core potentials (ECP) and their concomitant CEP-31G basis set.[22] This is equivalent to a double-ζ basis which is limited for a dianion like prephenate. Although substantially larger basis sets are easily used at the RHF level, the larger basis sets lead to intractable calculations for the excitation energies, which are obtained by solving the complete active space self-consistent-field (CASSCF) wave function for an active space that distributes 16 electrons in 11 orbitals. The in vacuo excitation energies are obtained by averaging the state density in the CASSCF so that the weight of the ground state equals that of all the other states. One test of the accuracy is the calculation of the electronic spectrum of phenyl pyruvate for a two-state average density CASSCF. The in vacuo excitation energy for a two-state CASSCF is 333 nm, shifted slightly to 324 nm in a PCM water continuum.[23] This is very good agreement with the reported absorption for phenyl pyruvate around 320 nm. All transition probabilities are obtained in the dipole approximation.

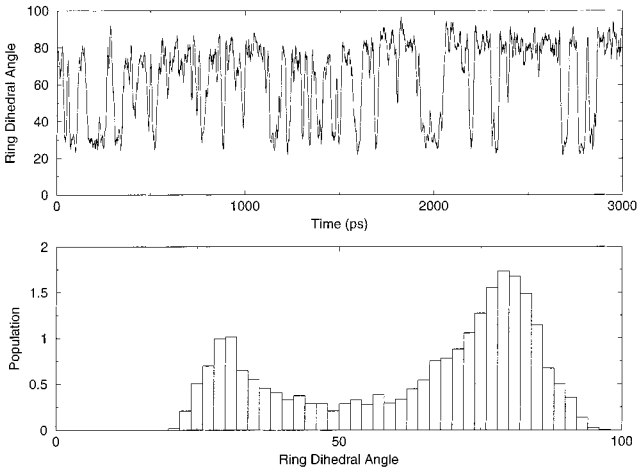

Figure 3. (a) Value of the dihedral angle, H(20)−C(6)−C(5)−H(21), plotted versus time for the duration of the dynamics run. (b) Histogram of the dihedral angles found in part a.

Experiment. Monofunctional CM from *B. subtilis*, recombinantly expressed in *E. coli*, was used to convert chorismate stoichiometrically to prephenate, as described previously.[12] The free acid form of chorismic acid (Sigma Chemical, St. Louis, MO) was used without further purification. Quantitation of chorismate was performed by measuring absorbance at 274 nm (absorption coefficient $\epsilon_{274} = 2700$ M^{-1} cm^{-1}). The reaction buffer consisted of 25 mM Tris (tris[hydroxymethyl]-aminomethane) buffer adjusted to pH 8.0 with HCl. Conversion of chorismate to prephenate was monitored using a Beckman DU 650 spectrophotometer. Scans of prephenate were recorded when conversion was complete as noted by a stable spectrum. The amount of chorismate mutase was in the nanomolar range and any absorbance due to chorismate mutase was subtracted from the final prephenate scans. Scans from 200 to 400 nm of prephenate in the concentration range of 0.1 to 2.0 mM were performed. Positive identification of prephenate as the product of chorismate + chorismate mutase has been previously performed by HPLC [12] and enzymatic assays.[24]

Results

Sampling and Energetics. Detailed analysis and clustering of the molecular dynamics run shows the presence of two main conformers, differing mostly on the ring puckering, and on the distance between the OH and the COO$^-$ attached to the ring. Figure 1 shows these two conformers, which we have called loose (a) (OH and COO$^-$ independently solvated) and tight (b) (H bond between OH and COO$^-$). Although the simulation was done in explicit water molecules, they are not shown in this figure. Figure 3a shows the value of the dihedral angle between atoms H(20)−C(6)−C(5)−H(21) along the dynamics run (the numbers refer to those in Figure 2). This angle is double valued, with the system spending a large amount of time at both 30° and 80°. A low value for the dihedral angle corresponds to the tight conformation and large values correspond to the loose conformation. Figure 3b presents a histogram of the dihedral values shown in Figure 3a. As can be seen, the loose conformation is preferred over the tight conformation.

Since the transitions between these two forms occur very rapidly in the subnanosecond time scale, and hence a large number of transitions are captured within the simulation time, we can be assured that the degree of freedom corresponding to this dihedral angle is thermalized. Under that condition, we can compute a free energy difference between the two conformers, at 300 K, by inversion of the histogram curve.

(21) Schmidt, M. W.; Baldridge, K. K.; Boatz, J. A.; Elbert, S. T.; Gordon, M. S.; Jensen, J. H.; Koseki, S.; Matsunaga, N.; Nguyen, K. A.; Su, S. J.; Windus, T. L.; Dupuis, M.; Montgomery, J. A. *J. Comput. Chem.* **1993**, *14*, 1347−1363.

(22) Stevens, W. J.; Basch, H.; Krauss, M. *J. Chem. Phys.* **1984**, *81*, 6026−6033.

(23) Cammi, R.; Tomasi, J. *J. Comput. Chem.* **1995**, *16*, 1449−1458.

(24) Kishore, N.; Holden, M. J.; Tewari, Y. B.; Goldberg, R. N. *J. Chem. Thermodyn.* **1999**, *31*, 211−227.

$$\Delta G_{\text{loose-tight}} = -0.6 \ln(N_{\text{loose}}/N_{\text{tight}}) = (-0.3 \pm 0.1) \text{ kcal/mol}$$

The error bars are estimated by halving the data set in Figure 3a and recomputing the free energies for both halves.

Ab initio calculations were also done on these conformers. Initially, in vacuo optimizations were performed and their energies computed as described in the methods section. We were unable to converge to an optimized structure for this dianion by solvating with the polarized continuum method (PCM).[23] Energies were computed, however, for the solvated optimized in vacuo conformer, using a PCM analysis with the default conditions in GAMESS[21] for continuum water. Table 3 presents the values of the relative energies for the two conformers. Zero is assigned to the lowest energy conformer at that particular level of calculation.

Both the classical and the quantum calculation predict that the lowest energy conformer in solution is not the one with the strong intramolecular H bond but the one where the two polar groups are instead independently solvated by water. The classical MD simulation predicts an energy difference of 0.3 kcal/mol while the QM PCM calculation provides a value of 0.1 kcal/mol with both methods favoring the loose conformer. Even though the PCM result has a large error associated with it, we are mostly interested in the fact that the energy difference between tight and loose is now much closer to zero, and not the 7.4 kcal/mol found in vacuo.

To identify the chromophore for the transition between the ground and first excited state, each of these states were partially optimized at the CASSCF level with 25 CASSCF iterations. The structure of the CASSCF ground state of the diaxial conformer does not change qualitatively from the RHF-optimized structure; the CO−COO dihedral angle is still quite large at 47°. The excited state geometry is substantially shifted with an increase in the carbonyl bond distance from 1.24 to 1.41 Å and the chromophore CO−COO dihedral angle reduced to 10°. This calculation identifies the chromophore as localized in the $CO-COO^-$ moiety.

Hence, we investigated the fluctuations for the dihedral angle comprised of atoms O(16)−C(8)−C(10)−O(12,13). The latter atom is picked so as to keep the angle between −180 and 180° excluding full 180° rotations that are equivalent because of symmetry. Figure 4 shows a histogram of that dihedral angle during the MD simulation.

The average and standard deviation are −10° and 27°, with the deviation from zero due to the presence of the large ring. In a vacuum the dihedral angle is substantially larger, ranging from 40° to 60°, due to the repulsion between the carbonyl and carboxylate charges which shielded in solution.

The wide distribution of this angle can be understood by studying the model compound $H-CO-COO^-$ by ab initio methods. An in vacuo estimate of the barrier for rotation around the CO−COO dihedral angle at an MP2 level (6-31G basis set) gives a value for the barrier of only 1.35 kcal/mol, very accessible at room temperature, producing large fluctuations.

Since this molecule is very flexible, with at least two conformers populated in explicit solvent, a single point calculation for the excitation electronic spectrum would not have provided the full picture, and a proper comparison with experiment would not have been possible. To obtain a more complete description of the system, we computed the electronic spectrum for a number of snapshots along the classical dynamics run. In previous work, another group[14,25] computed excitation spectra for rigid nonpolar molecules in polar solvents using semiempirical methods applied to uncorrelated frames from a Monte Carlo run. We instead use the results from the classical molecular dynamics simulations as a provider of sampling statistics. We pick particular conformations, perform quantum mechanical calculations of the electronic spectrum, and post-weight the results according to the relative abundance of the conformation during the classical MD runs. We use the angular distributions shown in Figures 3 and 4 as guides to pick structures. Six frames are chosen from each of the tight and loose conformations (Figure 3). Of those 6 frames, we chose 3 for sampling from Figure 4, according to their $CO-COO^-$ angle. One conformation had a dihedral angle corresponding to the average of the distribution, and the other two were chosen with dihedrals according to the standard deviation in Figure 4. The final three frames chosen are frames with the same angles but from different time frames, to achieve better statistics.

Table 3. Relative Energies for the Loose and Tight Conformers, in kcal/mol, for Ab Initio In Vacuum and PCM Calculations

	energy (kcal/mol)	
	in vacuo	PCM
loose	7.4	0.0
tight	0.0	0.1

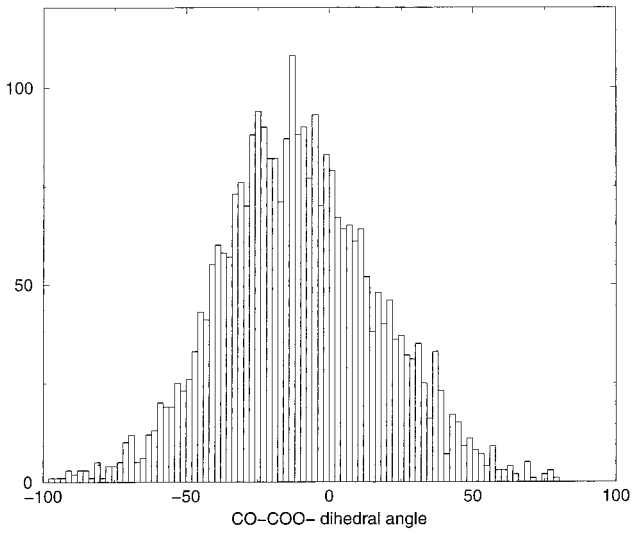

Figure 4. Histogram of the chromophore dihedral angle, O(16)−C(8)−C(10)−O(12,13), as found in the simulation.

Electronic Spectrum in Solution. The individual runs for the spectra were done as described in the methods section. Each run provided three excitation energies (wavelengths) and three associated transition intensities. We assigned (arbitrarily) a value of 1 to the intensity of the highest of the three transitions, and scaled all the others accordingly. After that, we scaled the transitions according to the weight of that particular snapshot during the classical MD simulation. Figure 5 presents the UV/vis spectrum computed theoretically and measured experimentally. The vertical lines correspond to the theoretical spectrum for the 12 conformers (3 lines for each) with intensities computed as described above. The experimental spectrum is presented as a dark line (with the highest energy intensity also normalized to 1). The measured absorption coefficients are $\epsilon_{274} = 250\ M^{-1}\ cm^{-1}$ and $\epsilon_{330} = 70\ M^{-1}\ cm^{-1}$.

There are two high-energy transitions predicted by theory, around 190 and 240 nm. The first one is also seen in the experiment, at around the same wavelength as the theory, and

(25) Coutinho, K.; Canuto, S.; Zerner, M. C. *Int. J. Quantum Chem.* **1997**, *65*, 885−891.

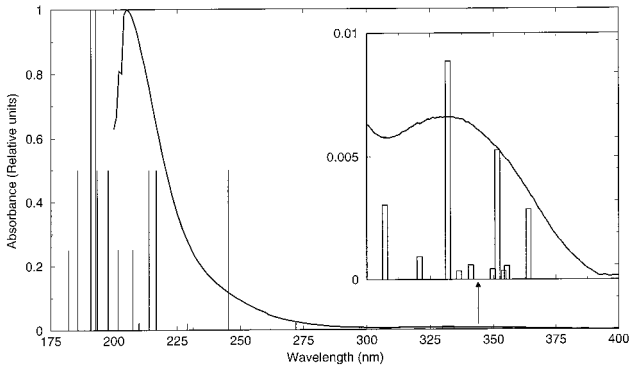

Figure 5. Comparison between experimental and theoretically derived spectra. The vertical lines correspond to the theoretical spectrum for 12 conformers (3 lines for each) with intensities computed as described in the main text. The experimental spectrum is presented as a dark line (with the highest energy intensity also normalized to 1). The measured extinction coefficients are $\epsilon_{274} = 250\ M^{-1}\ cm^{-1}$ and $\epsilon_{330} = 70\ M^{-1}\ cm^{-1}$. The inset shows the near-UV absorption in greater detail.

also with the (roughly) same broadening. The transition around 240 nm has a theoretical intensity of 0.01 with respect to the transition at 190 nm, and is probably experimentally masked under the broad 200 nm band. These two (190 and 240 nm) are $\pi \rightarrow \pi^*$ transitions localized in the C═C double bonds in the ring. As such they will be present (albeit with slightly different energies and intensities) in most molecules found in the aromatic acid pathways and will not be amenable for prephenate quantification or even qualitative differentiation between members of the pathway. The theoretical calculation predicts transitions slightly further to the blue than observed. We note that the experimental spectrum is not valid below 200 nm because of instrumental limitations. Since the excited states will have much larger dipole moments than the ground state, the solvatochromic shift would be to the red. The lack of agreement can be ascribed to the small basis set used in the calculation which will not properly represent these excited states. Not only are polarization functions neglected but there is no possibility of describing Rydberg mixing without including diffuse functions.

The transition predicted to be around 330 nm is unique to the CO−COO$^-$ chromophore, which is restricted to prephenate and phenyl pyruvate for the reactions associated with chorismate mutase. The inset in Figure 5 shows the expanded spectrum between 300 and 400 nm. The absorption scale is 0.01 of that corresponding to the 190 nm transition. The agreement between the theoretical and experimental spectrum in this region is excellent in three aspects: the transition energy, the overall shape and broadening, and the relative intensity of the band.

Electronic Spectrum in the Active Site. The prephenate bound in the active site is optimized with a first shell of polar and ionic residues. The prephenate is an all-electron molecule treated at the RHF level with the models of the protein residues represented by effective fragment potentials (EFP). The EFP replace the all-electron potentials in the quantum Hamiltonian.[16] EFP have been generated for all the residues necessary to construct the active site of chorismate mutase.[11] The initial structure for the optimization was obtained from the crystal structure of CM from *B. subtilis*.[13] Care in choosing these coordinates is required since there are 12 different active sites in the crystal structure. The active site is flexible in the region where substrate and product can enter or leave. Different motifs or arrangements of binding can be ascertained from the different active sites formed between different protein domains in the crystal structure, other crystal structures obtained with different molecules bound in the active site, or MD simulations starting from such structures. Only a single optimized structure for the prephenate is reported here, which agrees well with the observed structure in the active site formed between domains A and B.[13] This structure formally resembles the one in Figure 1a but, like the solution structure, the dihedral angle is small as may be expected in the cases where there is substantial shielding of the repulsions between the carbonyl and carboxylate bonds. The CASSCF solution for the enzyme model includes the EFP fields in the CASSCF matrix elements. The data for the computed spectrum inside the enzyme active site are presented in Table 4. The very ionic active site produces a very large shift (calculated to be blue) on the far-UV transitions. The transition with the largest oscillator strength is shifted more than 10000 cm^{-1}. Relatively little shift occurs with the lowest energy transition (330 nm → 339 nm), which is of the greatest interest since it could possibly be observed, allowing a probe of the electronic properties of the active site.

Table 4. Computed Wavelengths and Relative Absorption Intensities for the Electronic Spectrum on Prephenate Inside the Active Site of Chorismate Mutase

wavelength (nm)	intensity (relative units)
150	1
156	0.008
339	0.001

Conclusions

We can summarize three major conclusions. First, we present a real electronic spectrum for prephenate, as opposed to an alkaline solution spectra for prephenate reaction derivatives, and report the value $\epsilon_{330} = 70\ M^{-1}\ cm^{-1}$. The observed spectrum in the present article was obtained under conditions where the enzyme is stable. Second, the theoretical spectrum of the prephenate dianion in solution agrees very well with the experiment validating the MD/QM approach adopted here. By focusing on the conformational properties of the chromophore that we have identified with the spectral behavior, it is possible to select and weight a relatively few simulation snapshots for which quantum calculations of the spectrum need to be made. Since CASSCF calculations are required to obtain accurate excitation energies, examination of large numbers of snapshots would be intractable. Third, prephenate bound in the active site of chorismate mutase is predicted to absorb in the near-UV around 340 nm. Since the conformation of prephenate is quite restricted in the active site, the width of the band will be fairly narrow. A sensitive spectral method such as resonance Raman scattering could be used to determine the coupling of the prephenate to the active site.

Acknowledgment. We wish to thank Vincent L. Vilker for encouragement and discussion on this project as well as for careful reading and editing of the manuscript.

JA9945358